



OPEN

Construction and analysis of a ceRNA network and patterns of immune infiltration in chronic rhinosinusitis with nasal polyps: based on data mining and experimental verification

Jing-cai Chen^{1,4,5}, Qi-long Xing^{3,5}, Hui-wen Yang¹, Fan Yang¹, Yao Luo¹, Wei-jia Kong^{1,2}✉ & Yan-jun Wang^{1,2}✉

Recent studies have revealed the significant role of the competing endogenous RNA (ceRNA) network in human diseases. However, systematic analysis of the ceRNA mechanism in chronic rhinosinusitis with nasal polyps (CRSwNP) is limited. In this study, we constructed a competitive endogenous RNA (ceRNA) network and identified a potential regulatory axis in CRSwNP based on bioinformatics analysis and experimental verification. We obtained lncRNA, miRNA, and mRNA expression profiles from the Gene Expression Omnibus. After analysis of CRSwNP patients and the control groups, we identified 565 DE-lncRNAs, 23 DE-miRNAs, and 1799 DE-mRNAs by the DESeq2 R package or limma R package. Enrichment analysis of 1799 DE-mRNAs showed that CRSwNP was associated with inflammation and immunity. Moreover, we identified 21 lncRNAs, 8 miRNAs and 8 mRNAs to construct the lncRNA-miRNA-mRNA ceRNA network. A potential MIAT/miR-125a/IRF4 axis was determined according to the degree and positive correlation between a lncRNA and its competitive endogenous mRNAs. The GSEA results suggested that IRF4 may be involved in immune cell infiltration. The validation of another dataset confirmed that MIAT and IRF4 were differentially expressed between the CRSwNP and control groups. The area under the ROC curve (AUC) of MIAT and IRF4 was 0.944. The CIBERSORT analysis revealed that eosinophils and M2 macrophages may be involved in the CRSwNP process. MIAT was correlated with dendritic cells and M2 macrophages, and IRF4 was correlated with dendritic cells. Finally, to validate the key genes, we performed in-silico validation using another dataset and experimental validation using immunohistochemistry, immunofluorescence, and Western blot. In summary, the constructed novel MIAT/miR-125a/IRF4 axis may play a critical role in the development and progression of CRSwNP. We believe that the ceRNA network and immune cell infiltration could offer further insight into novel molecular therapeutic targets for CRSwNP.

Chronic rhinosinusitis (CRS) is a common chronic disease with a heavy socioeconomic burden¹. CRS is a multifactorial and heterogeneous group of sinus diseases characterized by inflammatory disease of the sinuses and mucosa of the nose². CRS is divided into CRS with nasal polyps (CRSwNP) and CRS without nasal polyps (CRSsNP) based on the presence or absence of polyps³. Clinically, CRSwNP is more recalcitrant and refractory than CRSsNP⁴. CRSwNP is histologically characterized by stromal tissue edema, formation of pseudocysts, and

¹Department of Otorhinolaryngology, Union Hospital, Tongji Medical College, Huazhong University of Science and Technology, Wuhan, China. ²Institute of Otorhinolaryngology, Union Hospital, Tongji Medical College, Huazhong University of Science and Technology, Wuhan, China. ³School of Computer Science and Technology, Huazhong University of Science and Technology, Wuhan, China. ⁴Department of Otorhinolaryngology, The First Affiliated Hospital, School of Medicine, Shihezi University, Shihezi, Xinjiang, China. ⁵These authors contributed equally: Jing-cai Chen and Qi-long Xing. ✉email: entwjkong@hust.edu.cn; yjwang@hust.edu.cn

significant immune cell infiltration⁵. CRSwNP is classically divided into two subsets: eosinophilic nasal polyps (ECRSwNP), which are found mainly in European and American patients and feature a Th2 signature, and noneosinophilic nasal polyps (non-ECRSwNP), which are found mainly in Asian patients with a mixed Th1/Th17 pattern of inflammatory response^{6,7}. Despite the great advances in functional endoscopic sinus surgery (FESS)⁸ and biologics^{9,10}, the treatment effect of CRSwNP is still unsatisfactory. There remained a surgical revision rate of 21%–29.9% for CRSwNP^{11,12}. While biologic therapy has been deployed with encouraging results, its use is constrained by high costs and the risk of anaphylaxis^{13,14}. Recently, accumulating studies have demonstrated that sinonasal epithelial cell barrier defects, increased exposure to pathogenic and colonized bacteria, and dysregulation of the host immune system are all thought to play prominent roles in disease pathogenesis^{15,16}. Although insights into the pathophysiology of CRSwNP have largely expanded over the last few decades, the precise etiology and mechanism of persistence are still unknown. Therefore, a more comprehensive understanding of the etiology and pathogenesis of CRSwNP helps to provide novel potential targets and clinical strategies for CRSwNP treatment.

Due to the development of sequencing and bioinformatics approaches, the important functions of noncoding RNAs (ncRNAs) have been identified in various aspects of cell biology and life processes. ncRNAs include microRNAs (miRNAs), long noncoding RNAs (lncRNAs), pseudogenes and circular RNAs, which were previously called “dark matter” or “junk RNA” because of their inability to encode proteins¹⁷. The study of dysregulated ncRNAs in diseases may provide a better understanding of the pathogenesis and hold promise for therapeutic strategies¹⁸. miRNAs are small noncoding RNAs (21–23 nucleotides) with a distinct capacity to negatively regulate target gene expression at the posttranscriptional level¹⁹. Increasing evidence indicates that miRNAs play a critical role in the pathogenesis of CRSwNP. A previous study revealed that the elevated level of miR-125b contributes to mucosal eosinophilia recruitment via the enhancement of type I interferon (IFN) expression in ECRSwNP tissue and may play a critical role in airway antiviral innate immunity by suppressing EIF4E-binding protein 1 (4E-BP1) expression²⁰. Furthermore, miR-124 participates in the regulation of the inflammatory response by mediating the expression of aryl hydrocarbon receptor (AHR) in CRSwNP²¹. Moreover, let-7a-5p has been revealed to regulate the inflammatory response by interacting with IL-6 through the Ras-MAPK pathway in CRSwNP²².

lncRNAs are a class of noncoding transcripts of >200 nucleotides that can regulate gene expression at the transcriptional or posttranscriptional level²³. The hypothesis of competing endogenous RNAs (ceRNAs) states that lncRNAs and mRNAs can interact with each other via miRNAs by forming a regulatory network²⁴. According to this theory, lncRNAs act as miRNA sponges by miRNA response elements (MREs) to absorb and bind miRNAs, which can modulate mRNA expression^{24,25}. The expression levels of these two RNA transcripts will have a positive relationship with each other²⁶. The effects of ceRNA networks depend on the identity, concentration, and subcellular distribution of the RNA and the miRNA species. However, lower levels of ncRNAs may also contribute to ceRNA sponge mechanisms, and even ceRNAs undergo marked rewiring between normal and pathological tissues^{27,28}. Many previous studies have confirmed that lncRNAs play essential roles in the proliferation, metastasis, drug sensitivity, and progression of tumors^{29,30}. Over the last few years, many studies have validated the ceRNA theory, as emerging evidence has verified that ceRNA crosstalk imbalance is associated with various diseases, especially cancers^{26–28}. Recent research has expanded to establish ceRNA networks in the field of inflammatory diseases³¹. Regarding chronic nasal inflammation, limited data about the role of lncRNAs have been reported, and only a limited number of lncRNAs have been discovered to be involved in its pathogenesis. Wang et al. found that lncRNA XLOC_010280 was highly expressed in ECRSwNP and played a vital role in eosinophilic inflammation by regulating CCL18 expression³². Another study indicated that lncRNA NEAT1 and its targets (miR-21 and miR-125a) were strongly correlated with the disease risk, severity, and inflammation of allergic rhinitis³³. However, to understand the roles of ceRNA networks in the pathogenesis and pathological conditions of CRSwNP, further research is needed.

In this study, we hypothesized that there were still a significant number of previously unexplored genetic differences between CRSwNP and normal tissues, especially with respect to ncRNA expression patterns. We screened several differentially expressed mRNAs, miRNAs and lncRNAs between CRSwNP patients and healthy controls from the Gene Expression Omnibus (GEO) dataset. Then, functional enrichment analysis was conducted to assess the functional role and potential mechanism of differentially expressed mRNAs in CRSwNP. Moreover, a ceRNA network was constructed to elucidate the interactions and potential crosstalk among the key lncRNAs, miRNAs, and mRNAs in CRSwNP. Finally, immune infiltration analysis was performed to study the relationship between the ceRNA axis (lncRNA and mRNA) and infiltrating immune cells to better understand the molecular immune mechanism during the development of CRSwNP. Subsequent to in-silico analysis, experimental validation of the key mRNAs was performed. Our study aimed to comprehensively assess the correlation of ceRNAs with the immune microenvironment, diagnostic biomarkers, and therapeutic targets in CRSwNP patients.

Materials and methods

Datasets selection and raw data preprocessing. The study was carried out in compliance with the guidelines of the Declaration of Helsinki. Figure 1 shows the workflow chart of this study. The Bioconductor package “GEOquery”³⁴ of R software (version 4.1.0, <http://r-project.org/>) was used to extract the CRSwNP expression profile datasets GSE136825³⁵, GSE36830³⁶, GSE179265³⁷ and GSE169376³⁸ from the Gene Expression Omnibus (GEO) database (<https://www.ncbi.nlm.nih.gov/geo/>). The mRNA and lncRNA data from GSE136825 and the miRNA data from GSE169376 were sorted into standardized original data for subsequent analysis. The GSE36830 dataset and GSE179265 dataset were applied to examine the expression of lncRNA and mRNA biomarkers as the validation cohort. The GSE36830 dataset was applied to analyze immune cell infiltration. The ensemble ID of samples was converted by using the HGNC symbol. Detailed information on the four datasets is shown in Table 1.

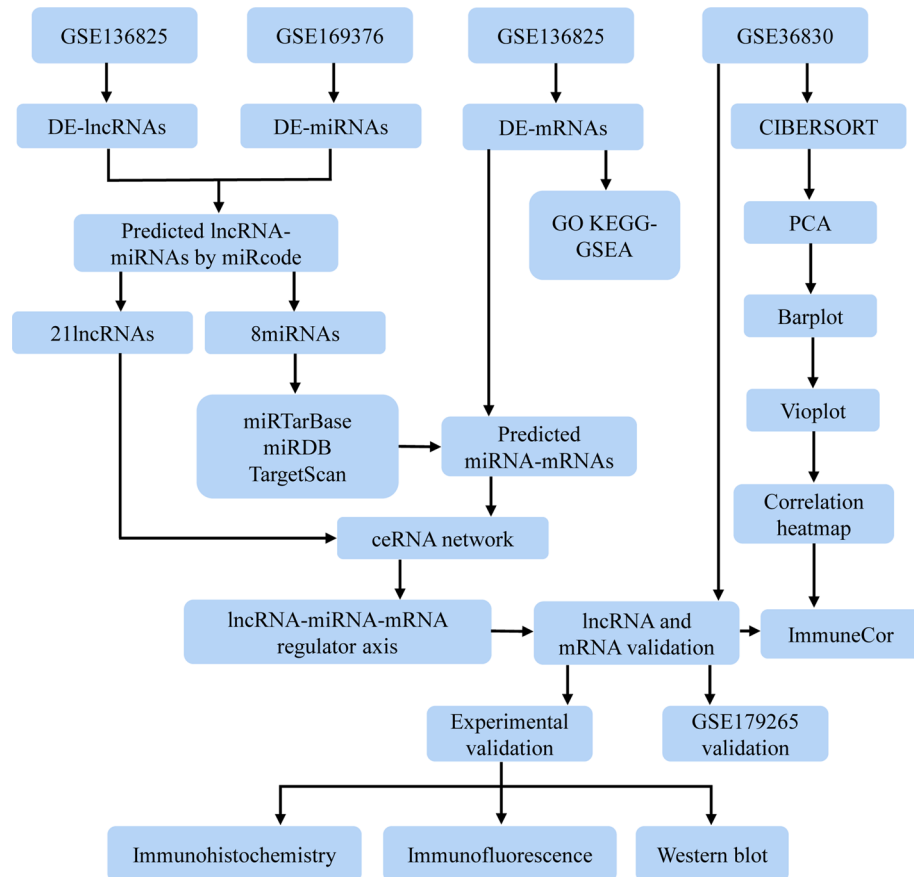


Figure 1. Flow chart of the study design.

Accession	Platform	Study type	Sample	CRSwNP/Control	RNA type
GSE136825	GPL20301	RNA-seq	NP/Control	42/28	mRNA/lncRNA
GSE36830	GPL570	Array	NP/Control	6/6	mRNA/lncRNA
GSE179265	GPL24676	RNA-seq	NP/Control	17/7	mRNA/lncRNA
GSE169376	GPL21572	Array	NP/Control	6/3	microRNA

Table 1. Details for GEO CRSwNP Data. CRSwNP chronic rhinosinusitis with nasal polyps; NP nasal polyp; GEO Gene Expression Omnibus.

Identification of differentially expressed genes (DEGs). We used the “DESeq2” package³⁹ to identify DEGs (DE-lncRNAs and DE-mRNAs) between nasal polyp samples and control samples. We considered that $|\log_2 FC|$ (absolute value of \log_2 in the fold change of gene expression) ≥ 1 and adjusted p value with a false discovery rate (FDR) < 0.05 were statistically significant. The “limma” package⁴⁰ was used to identify DE-miRNAs between nasal polyp samples and control samples, and FDR < 0.05 and $|\log_2 FC| \geq 1$ were defined as the criteria of significance. Then, heat maps and volcano plots were drawn using “pheatmap” and “ggplot2” packages of R software to indicate the DEGs.

Functional enrichment analysis. We used the R package “clusterprofiler”⁴¹ to analyze the Gene Ontology (GO) functional enrichment of DE-mRNAs. By functional enrichment analysis, we determined which biological process (BP), cellular component (CC) and molecular function (MF) were significantly (FDR < 0.05) enriched in both CRSwNP and control subjects during differentiation. The Kyoto Encyclopedia of Genes and Genomes (KEGG)-Gene Set Enrichment Analysis (GSEA) was searched for pathways at the significance level set at FDR < 0.05 ^{42,43}.

Construction of a ceRNA network. First, lncRNA-miRNA interactions were constructed based on DE-lncRNAs from miRcode (<http://www.mircode.org/>). The candidate target miRNAs were then compared with DE-miRNAs. Next, we used miRTarBase (https://mirtarbase.cuhk.edu.cn/~miRTarBase/miRTarBase_

2022/php/index.php), miRDB (<http://www.mirdb.org/>) and TargetScan (<http://www.targetscan.org/>) to predict miRNA-mRNA interactions by candidate target miRNAs. Then, we constructed a lncRNA-miRNA-mRNA ceRNA network and visualized it by Cytoscape software (version 3.8.2, <https://cytoscape.org/>⁴⁴). The Cytoscape plug-in cytoHubba was used to identify hub genes in this network. Correlations between the expression of the hub lncRNA and its competitive endogenous mRNAs were analyzed by Pearson correlation analyses.

Gene set enrichment analysis of the key mRNAs in the ceRNA network. Gene set enrichment analysis (GSEA) is a knowledge-based method for the translation of genome-wide expression profiles⁴³. We analyzed the pathways of the key mRNAs of the ceRNA network using GSEA. The cutoff criteria were NES > 2, FDR < 0.01, and *p* value < 0.01.

Validation of the ceRNA network. To verify the ceRNA network and our results, we used the “limma” package to identify DEGs of GSE36830, which included lncRNA and mRNA information from 6 CRSwNP patients and 6 control subjects. DEGs were screened by $|\log_2 \text{FC}| \geq 1$ and FDR < 0.05. Receiver operating characteristic (ROC) curves and the area under the curve (AUC) were used to measure the diagnostic performance of the lncRNAs, mRNAs, lncRNAs and mRNAs by GraphPad Prism Version 9.

Evaluation of immune cell infiltration. CIBERSORT is a deconvolution algorithm that uses gene expression signatures consisting of 547 genes to predict 22 immune cell phenotypes⁴⁵. We uploaded standard annotated gene expression data of GSE36830 to the CIBERSORT web portal (<http://cibersort.stanford.edu/>) and obtained the immune cell infiltration matrix. The samples were screened according to *p* value < 0.05. Then, we used the “ggplot2” package⁴⁶ to draw two-dimensional PCA maps and violin diagrams to visualize the differences in immune cell infiltration. The “corrplot” package⁴⁷ was used to draw a correlation heatmap to visualize the correlation of 22 types of infiltrating immune cells.

Correlation analysis between the ceRNA axis (lncRNA and mRNA) and infiltrating immune cells. Spearman correlation analysis was performed on lncRNAs, mRNAs of the ceRNA axis and infiltrating immune cells using the “ggstatsplot” package based on the lack of a linear relationship between genes and immune cells, and the gene distribution did not conform to a normal distribution. The “ggplot2” package was used to visualize the results.

In-silico validation. To validate the mRNA and lncRNA expression levels of the screened key genes between CRSwNP and control subjects, the validation dataset GSE179265 was used. The dataset included RNA-seq expression data from human nasal polyp samples (*n* = 17) and control samples (*n* = 7). The DEGs were assessed using the default settings of “EdgeR” package⁴⁸. DEGs were screened by $|\log_2 \text{FC}| \geq 1$ and FDR < 0.05. The expression of mRNA and lncRNA between CRSwNP and control subjects was analyzed by Student’s *t*-test, using GraphPad Prism version 9. The correlation between the mRNA and lncRNA was analyzed by Pearson correlation analyses using GraphPad Prism Version 9.

Experimental validation. Twenty four CRSwNP nasal polyps and twelve normal nasal mucosa tissue samples were obtained from the Department of Otorhinolaryngology, Union Hospital (Wuhan, China) and all subjects signed consent forms. Diagnosis of CRSwNP was made according to the current European Position Paper on Rhinosinusitis and Nasal Polyps 2020¹. All control patients were defined as those without CRS who were undergoing skull base surgery or endonasal surgery for anatomic abnormalities. This study was approved by Ethics Committee of Union Hospital, Tongji Medical College, Huazhong University of Science and Technology (20,220,343).

Immunohistochemistry and immunofluorescence. We fixed the nasal polyp tissues and control tissues in 4% paraformaldehyde and embedded it in a wax block. 5 μm sections were obtained from blocks, and the sections were dewaxed with xylene and hydrated in a graded ethanol series. The samples were then treated with 3% hydrogen peroxide solution for 10 min and further washed with PBS. Antigen retrieval was performed in TRIS-EDTA buffer (pH 9.0) using a microwave oven (900 W for 15 min). The blocked sections were incubated overnight at 4 °C with anti-IRF4 (1:300 diluted, rabbit polyclonal, YT2399, ImmunoWay Biotechnology, Plano, TX, USA) and CD68 (1:4000 diluted, Mouse Monoclonal, 66231-2-Ig, Proteintech) antibody. The next day, the sections were rinsed three times with PBS, and for immunohistochemistry, the slides were incubated with horseradish peroxidase (HRP)-linked secondary antibodies of two-step immunohistochemical detection kit (G1210-2, Servicebio, Wuhan, China), and the color was visualized with DAB (Servicebio, Wuhan, China). The percentage of positive epithelial cells was categorized into four grades: 0 for < 5% positive cells, 1 for 6%–25% positive cells, 2 for 26%–50% positive cells, 3 for 51%–75% positive cells, and 4 for > 75% positive cells. Staining intensity of cytoplasm and nuclei was categorized into three grades: 0, no staining; 1, slightly yellow (weak) staining; 2, brown-yellow (moderate) staining; and 3, brown (strong) staining. The final score was the multiplication of the percentage and intensity scores (overall score range, 0–12). The positive inflammatory cells were presented as numbers per high-power field (HPF).

For immunofluorescence histochemistry, the sections were incubated with Alexa Fluor 488 Donkey Anti-Rabbit IgG (H+L) (diluted 1:300) and Alexa Fluor 647 Donkey Anti-Mouse IgG (H+L) (diluted 1:300) for 1 h. After four washes, the slides were incubated with DAPI (4,6-diamidino-2-phenylindole, G1012-100ML,

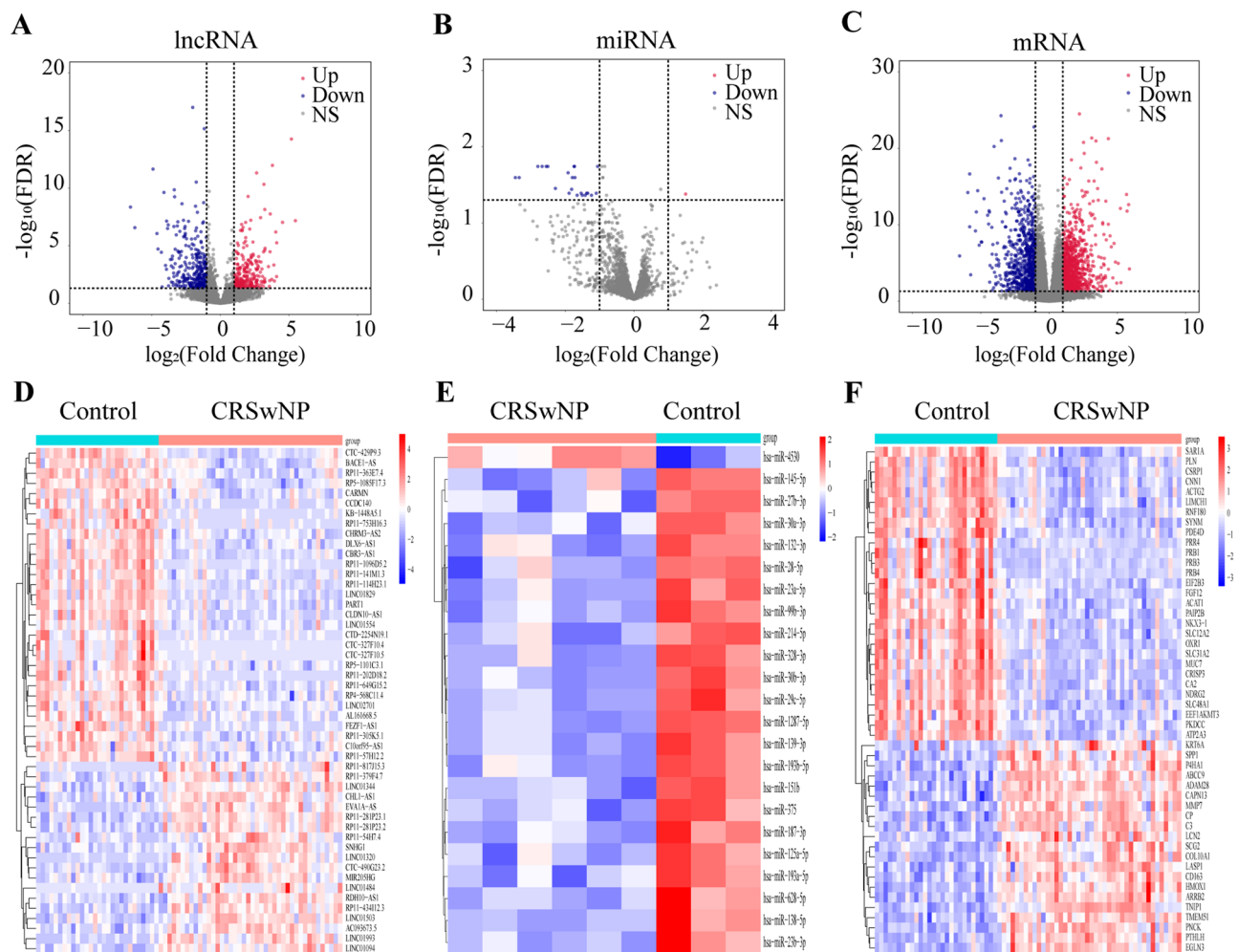


Figure 2. Differentially expressed gene analysis. Red indicates upregulation, blue indicates downregulation, and black indicates no significant difference. (A) Volcano map of significantly differentially expressed lncRNAs. (B) Volcano map of significantly differentially expressed miRNAs. (C) Volcano map of significantly differentially expressed mRNAs. (D) Hierarchical clustering heatmap of the top 50 differentially expressed lncRNAs. (E) Hierarchical clustering heatmap of all differentially expressed miRNAs. (F) Hierarchical clustering heatmap of the top 50 differentially expressed mRNAs. Hierarchical clustering heatmap was generated using the R package “pheatmap” (version 1.0.12. <https://CRAN.R-project.org/package=pheatmap>).

Servicebio, Wuhan, China) for the staining of nuclei. Images were captured with a confocal laser scanning microscope (Nikon-A1-Si, Nikon Corporation).

Western blotting. Total proteins were extracted from CRSwNP tissues and control tissues using RIPA lysis buffer (Beyotime Biotechnology, China) containing phosphatase inhibitors and PMSE, followed by concentration detection with the BCA protein assay kit. 20 μg protein were separated by electrophoresis using 10% sodium dodecyl sulfate polyacrylamide gels and then transferred to polyvinylidene difluoride (PVDF) membranes for incubation with anti-IRF4 (1:1000 diluted, rabbit polyclonal, YT2399, ImmunoWay Biotechnology, Plano, TX, USA) antibody. After three washes with TBST, membranes were incubated with horseradish peroxidase-conjugated goat anti-rabbit IgG (diluted 1:5000) for 1 h at room temperature, then washed with TBST buffer three times. An ECL detection reagent (G2014-50ML, Servicebio, Wuhan, China) was used to visualize the membranes. The relative expression level of proteins was represented in the ratio of the target protein and GAPDH using ImageJ software (National Institutes of Health, USA).

Statistical analysis. All data were expressed as the mean \pm SEM. Analyses were performed using the Student’s t test and the Mann–Whitney test as appropriate, using GraphPad Prism Version 9. Differences were considered significant at p value < 0.05 .

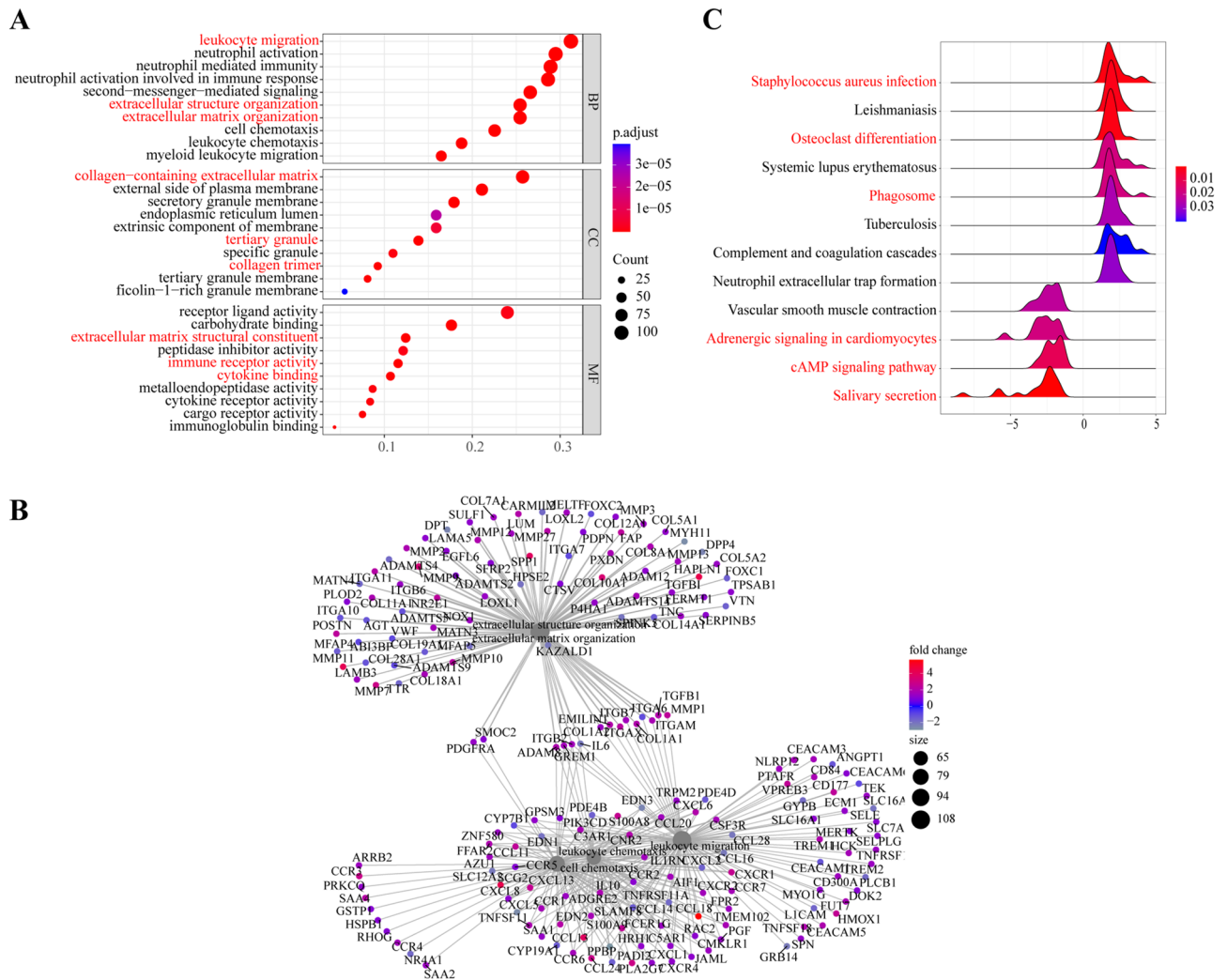


Figure 3. Functional enrichment analysis of DE-mRNAs. **(A)** GO analysis of DE-mRNAs in biological process (BP), molecular functions (MF) and cellular component (CC). **(B)** Gene symbols and interactions of the significantly DE-mRNAs in biological process (BP) are shown. **(C)** KEGG-GSEA pathway analysis of DE-mRNAs. GO, Gene Ontology; KEGG, Kyoto Encyclopedia of Genes and Genomes (www.kegg.jp/kegg/kegg1.html); GSEA, Gene Set Enrichment Analysis.

Results

Differentially expressed RNAs (DE-RNAs) in CRSwNP. Using a cutoff threshold of $|\log_2 FC| \geq 1$ and $FDR < 0.05$ for the 42 CRSwNP tissues compared with 28 control samples, we identified 565 DE-lncRNAs (267 upregulated and 298 downregulated), 23 DE-miRNAs (1 upregulated and 22 downregulated), and 1799 DE-mRNAs (1071 upregulated and 728 downregulated). All DEGs were highlighted in volcano plots (Fig. 2A–C). Hierarchical clustering analysis revealed the expression patterns of the top 50 DE-mRNAs and DE-lncRNAs, and all DE-miRNAs were capable of distinguishing CRSwNP subjects from control subjects (Fig. 2D–F).

Functional enrichment analysis. Gene Ontology (GO) analysis was applied to test the biological function of the identified genes. A total of 972 GO terms were enriched, and the top 10 enriched GO terms of each group according to FDR are displayed. DE-mRNAs were enriched in leukocyte migration, extracellular structure organization and extracellular matrix organization in BP, collagen-containing extracellular matrix, tertiary granule and collagen trimer in CC, and immune receptor activity, cytokine binding and extracellular matrix structural constituent in MF (Fig. 3A). Figure 3B shows the gene symbols and their interactions in BP of DE-mRNAs. The network presented numerous genes, such as CCL18, CCL13, MMP11, SCG2, HAPLN1, and SPPI1, that were significantly differentially expressed in CRSwNP. Moreover, *Staphylococcus aureus* infection, osteoclast differentiation, and phagosome were upregulated, while the cAMP signaling pathway, salivary secretion and adrenergic signaling in cardiomyocytes were downregulated by KEGG-GSEA (Fig. 3C).

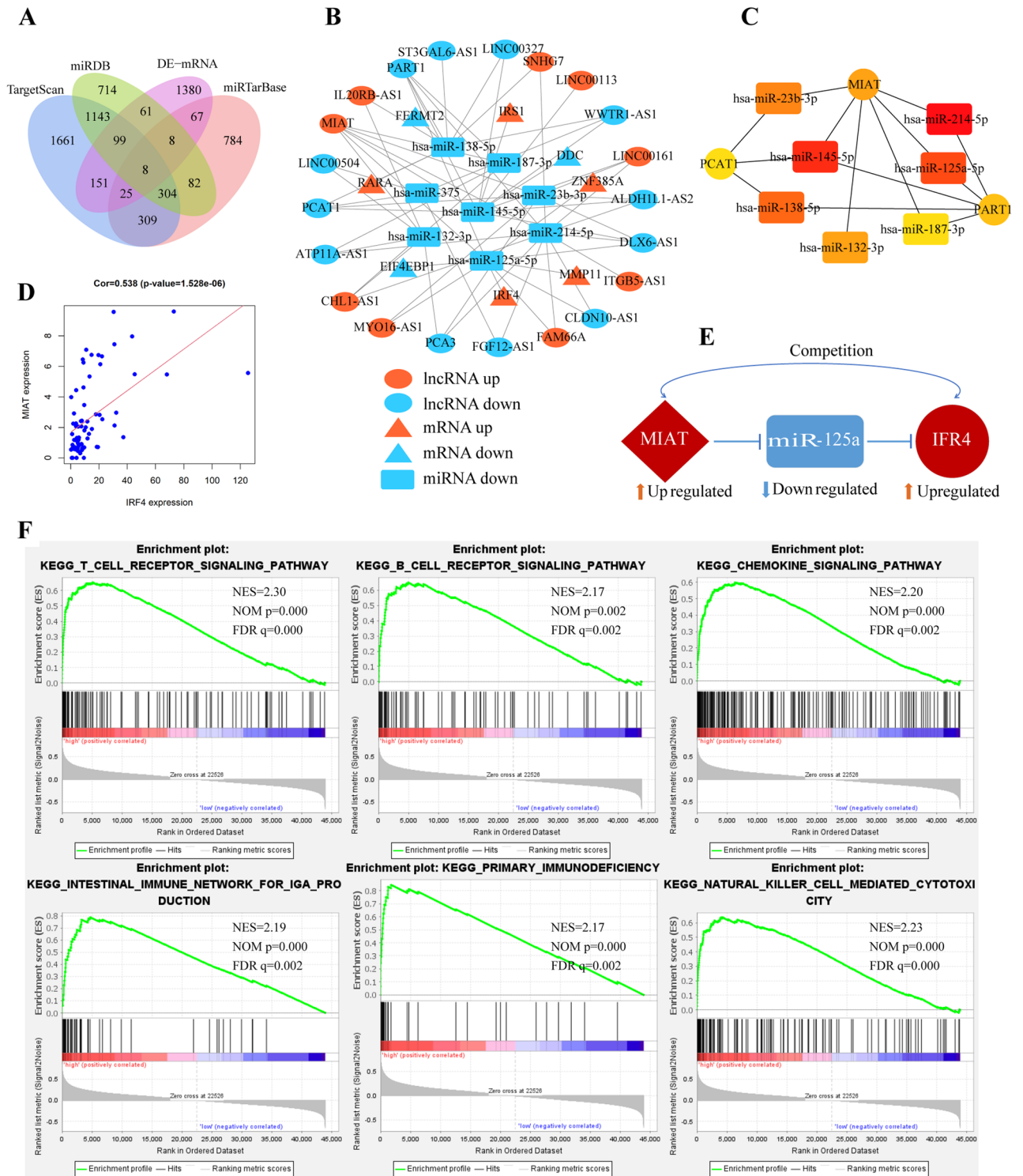


Figure 4. A potential lncRNA-miRNA-mRNA ceRNA network was constructed. **(A)** Venn diagram of predicted target mRNAs and DE-mRNAs. **(B)** The ceRNA network derived from DEGs in CRSwNP. The ellipses, round rectangles and triangles represent lncRNAs, miRNAs and mRNAs, respectively. Upregulation is represented by red nodes, while downregulation is represented by blue nodes. **(C)** Ten hub genes in this network using the Cytoscape plug-in cytoHubba. **(D)** Correlation analysis between MIAT and IRF4 in CRSwNP. **(E)** The MIAT/miR-125a/IRF4 regulatory axis perfectly conformed to the ceRNA hypothesis. **(F)** Gene set enrichment analysis of IRF4. DE-mRNA, differentially expressed mRNA; NES, normalized NS; FDR, false discovery rate.

Name	Regulation	Degree
hsa-miR-214-5p	Down	13
hsa-miR-145-5p	Down	11
hsa-miR-125a-5p	Down	10
hsa-miR-138-5p	Down	9
hsa-miR-23b-3p	Down	7
MIAT	Up	6
hsa-miR-132-3p	Down	6
PART1	Down	5
PCAT1	Down	4
hsa-miR-187-3p	Down	4

Table 2. The result of hub genes using Cytoscape plug-in Cytohubba.

Construction of a ceRNA network and validation of lncRNAs and mRNAs. First, we employed miRcode to predict lncRNA-miRNA interactions based on DE-lncRNAs. The overlapping target miRNAs between candidate target miRNAs and DE-miRNAs were chosen. We obtained 8 miRNAs and 21 lncRNAs (56 lncRNA-miRNA pairs). Next, miRTarBase, miRDB and TargetScan were utilized to predict miRNA-mRNA interactions. Then, we chose the overlapping target mRNAs (8 mRNAs) by analyzing the predicted target mRNAs and DE-mRNAs (Fig. 4A). Finally, a lncRNA-miRNA-mRNA ceRNA network was constructed with 21 lncRNAs, 8 miRNAs and 8 mRNAs, as shown in Fig. 4B. The Cytoscape plug-in cytoHubba was utilized to determine the hub regulatory network (Fig. 4C) (Table 2). The results showed that only lncRNA MIAT was chosen according to degree > 5 as the hub lncRNA. According to the ceRNA theory, the expression of lncRNAs and mRNAs are coexpression relationships. Pearson correlation coefficients were used to identify mRNA-lncRNA pairs based on the expression values of competing mRNA-lncRNA pairs. IRF4 expression was moderately positively correlated with MIAT expression ($r = 0.538$, p value < 0.05) (Fig. 4D), while other mRNAs were not correlated with MIAT. Therefore, we consider the MIAT/miR-125a/IRF4 subnetwork to be a potential key regulatory axis in the ceRNA network, which may play a critical role in the pathogenesis of nasal polyps (Fig. 4E).

We performed GSEA to identify the pathways associated with IRF4. The expression of IRF4 was used as the basis of sample classification. GSEA showed that the T-cell receptor signaling pathway, B-cell receptor signaling pathway, chemokine signaling pathway, and natural killer cell-mediated cytotoxicity were significantly positively related (Fig. 4F).

To test the robustness of the lncRNA and mRNA biomarkers for CRSwNP, MIAT and IRF4 were applied to the independent GSE36830 dataset. As shown in Fig. 5A, the expression of MIAT (p value = 0.002) and IRF4 (p value = 0.041) was significantly upregulated in CRSwNP, which was consistent with our analyzed result. The diagnostic accuracy of MIAT and IRF4 was assessed using ROC curve analysis (AUC of MIAT: 1.000; AUC of IRF4: 0.861; AUC of MIAT and IRF4: 0.944) (Fig. 5B).

Immune cell infiltration results. By using the CIBERSORT algorithm, we observed a difference in immune infiltration between CRSwNP tissues and normal tissues of 22 subpopulations of immune cells. Based on the criteria of p value < 0.05, 12 samples (6 CRSwNP samples and 6 control samples) were all included. As shown in Fig. 5C,D, the fraction of immune cells varied significantly among the CRSwNP and control samples. Then, the violin plot of the immune cell infiltration difference showed that eosinophils and M2 macrophages infiltrated more in CRSwNP samples than normal control samples. However, plasma cells and activated mast cells were relatively lower (Fig. 6A). Furthermore, a correlation heatmap of the 22 types of immune cells revealed that resting NK cells and naive CD4+T cells showed the most synergistic effect. Additionally, activated mast cells and resting mast cells showed the most competitive effect (Fig. 6B). Together, these results indicated that aberrant immune infiltration may have important clinical value in CRSwNP.

Correlation analysis between the ceRNA axis (lncRNA and mRNA) and infiltrating immune cells. Correlation analysis showed that MIAT was positively correlated with M2 macrophages ($r = 0.874$, p value < 0.001) and resting dendritic cells ($r = 0.698$, p value = 0.012) and negatively correlated with plasma cells ($r = -0.720$, p value = 0.008) (Fig. 7A). IRF4 was positively correlated with resting dendritic cells ($r = 0.606$, p value = 0.037) and negatively correlated with activated NK cells ($r = -0.741$, p value = 0.006) (Fig. 7B). Therefore, these findings further support that the ceRNA axis is closely correlated with the immune infiltration level in CRSwNP, suggesting that the ceRNA regulatory network might be a novel target for the diagnosis and treatment of CRSwNP.

Validation

In-silico validation. We performed in-silico validation by using another dataset. In GSE179265, the expression of MIAT (p value = 0.0003) and IRF4 (p value = 0.0042) significantly up-regulated in the nasal polyp group than control group (Fig. 8A,B). The expression of IRF4 was positive correlation with lncRNA MIAT ($r = 0.794$, p value < 0.05) (Fig. 8C).

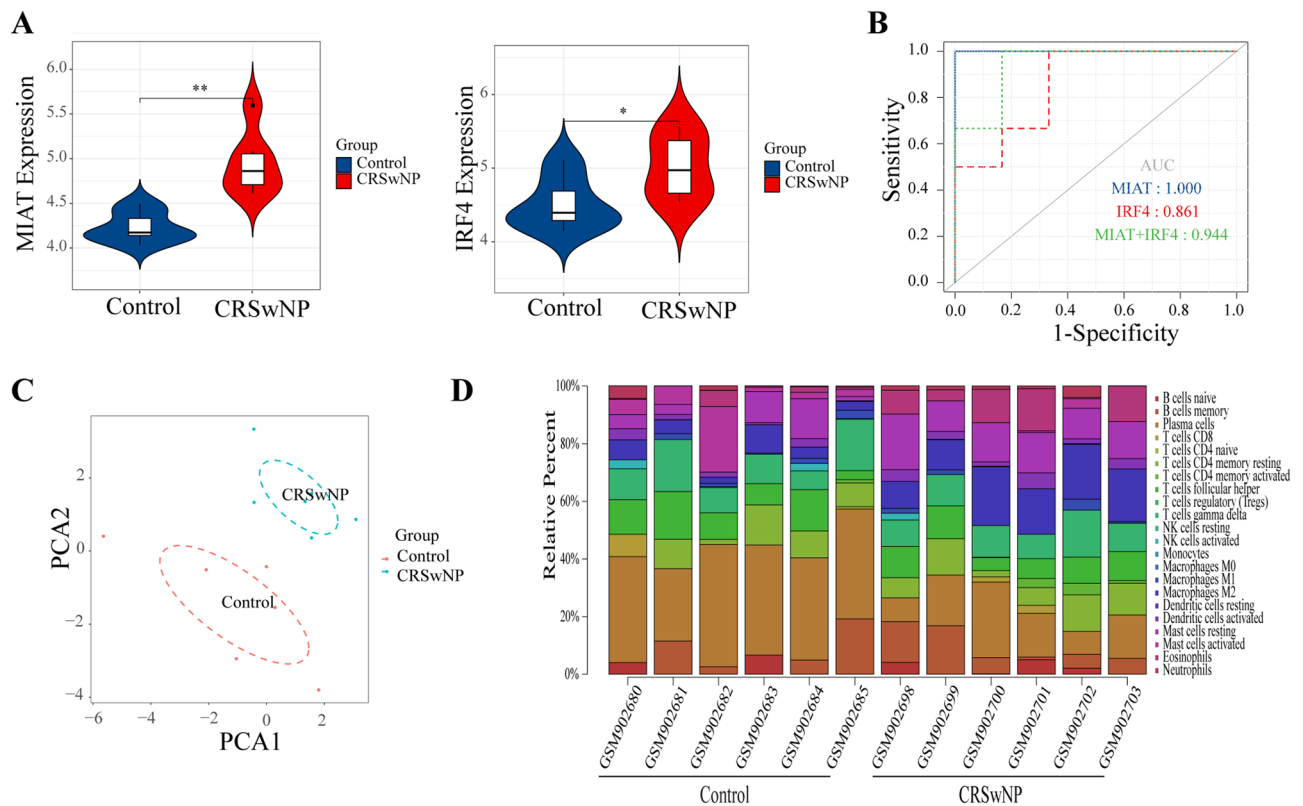


Figure 5. GSE36830 validation and evaluation of immune cell infiltration. **(A)** Expression pattern of MIAT and IRF4 in CRSwNP and control subjects. **(B)** The ROC curves of MIAT (blue dotted line), IRF4 (red dotted line), MIAT and IRF4 (green dotted line). **(C)** PCA cluster plot of immune cell infiltration performed on all samples. **(D)** Bar charts of 22 immune cell proportions in the CRSwNP and control groups. ROC, receiver operating characteristic; AUC, area under the receiver operating characteristic curve. * p value < 0.05, ** p value < 0.01.

Experimental validation. Immunohistochemistry showed that IRF4 is expressed in mucosal epithelium and macrophages of lamina propria in nasal polyp tissues, and the numbers of IRF4 positive cells in epithelium and lamina propria were marked enhanced in nasal polyp tissues in comparison with those in control tissues (Fig. 9A). Confocal showed co-localization of IRF4 and CD68 (M2 macrophage marker) in lamina propria (Fig. 9B). Western blot results showed that the expression of IRF4 in nasal polyps was significantly higher than that in the control group (p value < 0.0001) (Fig. 9C).

Discussion

In the past, many studies have investigated the molecular mechanisms of nasal polyp formation and growth^{22,49–51}. However, most studies have focused on elucidating the molecular mechanism involved in mRNAs and miRNAs^{52,53}. With the rapid development of next-generation sequencing, long noncoding RNAs (lncRNAs) longer than 200 nucleotides in length have been discovered. This novel transcript has been demonstrated to play important roles in a wide range of biological processes in humans. Recent studies have demonstrated the vital role of lncRNAs in CRSwNP, and some of these lncRNAs may be potential biomarkers for diagnosis and therapeutic targets^{32,54}. The competing endogenous RNA (ceRNA) hypothesis proposed by Salmena et al. in 2011 pointed to lncRNAs acting as endogenous molecular sponges that competitively bind miRNAs via shared MREs with reverse complementary binding seed regions to indirectly regulate mRNA expression levels²⁴. Although a number of studies have indicated the involvement of ceRNA crosstalk in tumorigenesis³⁵, progression⁵⁶ and metastasis⁵⁷ of cancers, there is still a paucity of studies on the comprehensive analysis of the lncRNA-miRNA-mRNA ceRNA network in CRSwNP.

CRSwNP is characterized by tissue remodeling (with collagen and fibrin deposition) and inflammation and has combinations of Th1, Th17 and/or Th2 inflammatory cytokines^{58,59}. Dysregulation of the immune response, epithelial barrier dysfunction, microbial colonization, and environmental exposures have been reported as etiologic factors of CRSwNP^{5,60}. The dysregulation of the host immune system has also been thought to play prominent roles in the pathogenesis of CRSwNP¹⁵. Defects in the innate immune function of the upper airway epithelium have been reported to play a role in the initial inflammatory response leading to CRSwNP. Subsequent recruitment and activation of eosinophils, neutrophils, mast cells, basophils, and innate lymphoid cells could further contribute to a chronic inflammatory response and directly activate adaptive immune cells, including T and B cells⁶¹. Therefore, finding specific diagnostic markers and analyzing the pattern of CRSwNP immune cell infiltration have profound significance for the treatment of CRSwNP patients.

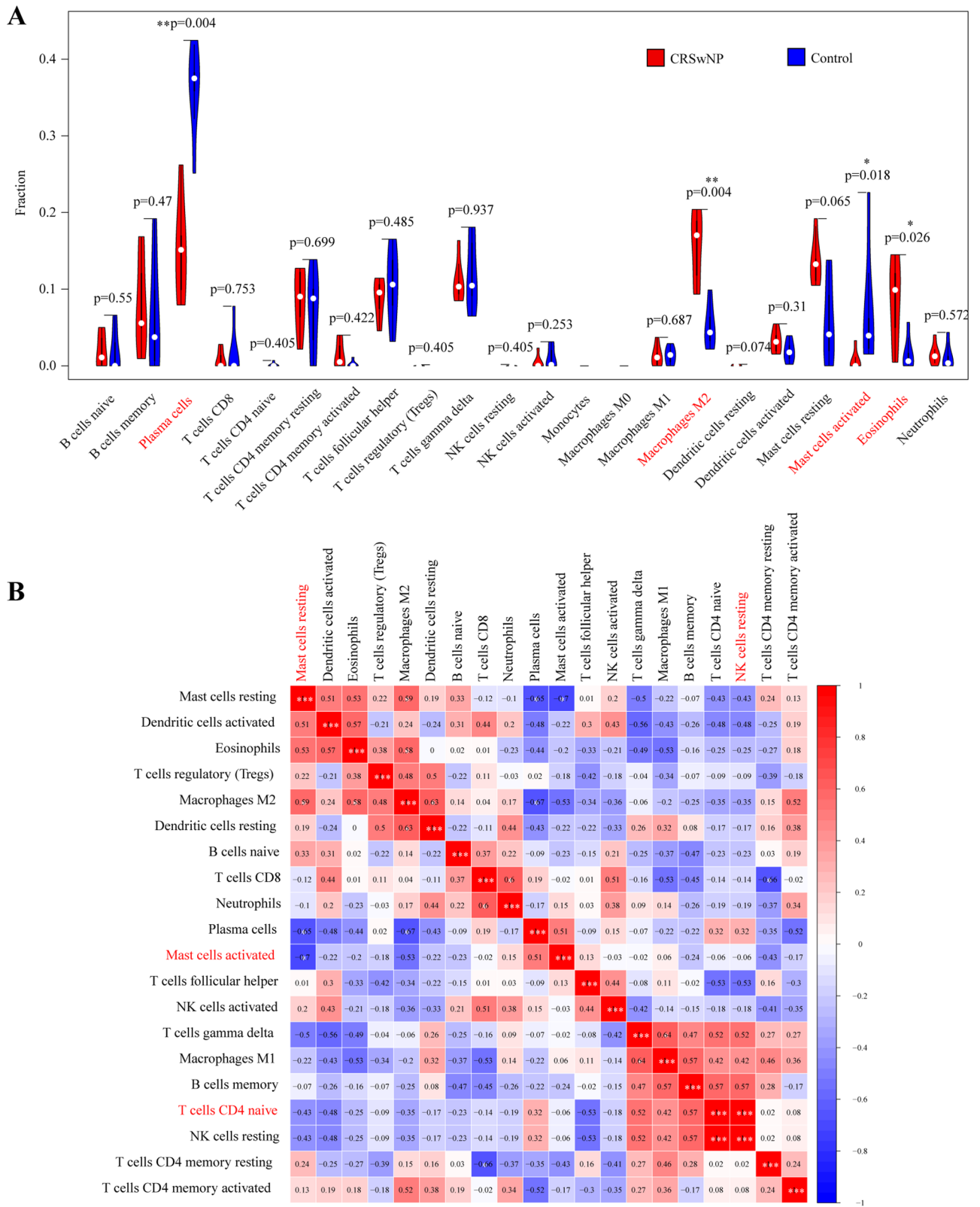


Figure 6. The landscape of immune infiltration between CRSwNP and normal controls. **(A)** Violin diagram of the proportion of 22 types of immune cells. **(B)** Correlation heatmap of 22 types of immune cells. Red: positive correlation; blue: negative correlation. Correlation heatmap were generated using R package “corrplot” (version 0.84. <https://github.com/taiyun/corrplot>). * p value < 0.05, ** p value < 0.01, *** p value < 0.001.

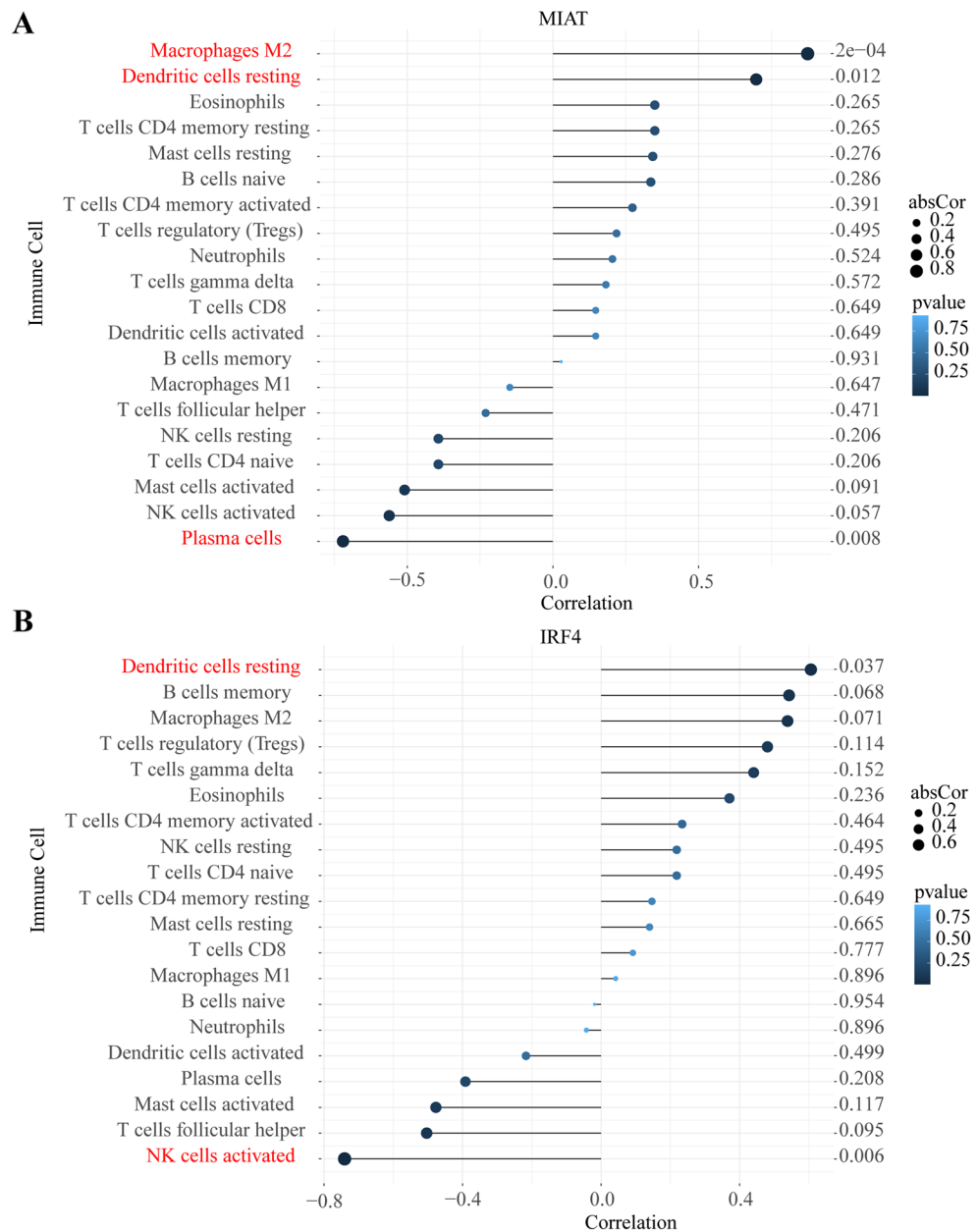


Figure 7. Correlation between the ceRNA axis (MIAT and IRF4) and infiltrating immune cells. **(A)** Correlation between MIAT and infiltrating immune cells. **(B)** Correlation between IRF4 and infiltrating immune cells.

In the present study, we integrated four GEO datasets for CRSwNP, which included mRNA, lncRNA, and microRNA expression. First, we identified 565 DE-lncRNAs (267 upregulated and 298 downregulated), 23 DE-miRNAs (1 upregulated and 22 downregulated), and 1799 DE-mRNAs (1071 upregulated and 728 downregulated) in CRSwNP samples from the GEO database (Fig. 2A–C). Then, by functional enrichment analysis, these DE-mRNAs were significantly enriched in leukocyte migration, extracellular structure organization and extracellular matrix organization (BP) (Fig. 3A). Notably, CCL18, CCL13, MMP11, SCG2, HAPLN1, and SPP1 were significantly upregulated genes in BP (Fig. 3B). CCL18 and CCL13 are chemokines; furthermore, CCL18 is regulated by Th2 cytokines and is significantly upregulated in CRSwNP⁶². Matrix metalloproteinase 11 (MMP11) belongs to the matrix metalloproteinase (MMP) family. MMP11 plays a role in different biological processes, such as embryonic tissue remodeling, extracellular matrix (ECM) remodeling, epithelial growth, and wound healing⁶³. Secretogranin II (SCG2) has been shown to suppress endothelial cell apoptosis and enhance angiogenesis of endothelial cells to facilitate neo-vascularization and rapid wound repair and regeneration⁶⁴. Hyaluronan and proteoglycan link protein 1 (HAPLN1) and secreted phosphoprotein 1 (SPP1) are associated with ECM structure, composition, and mechanics in cancer^{65,66}. Subsequent KEGG-GSEA pathway enrichment analysis also suggested that those DE-mRNAs may be involved in various pathways related to CRSwNP, such as *Staphylococcus aureus* infection, osteoclast differentiation, and phagosomes (Fig. 3C). CRSwNP patients are significantly more likely

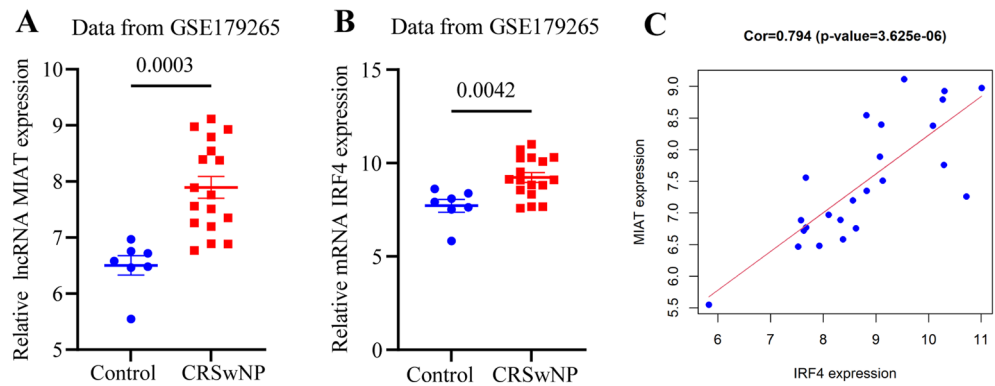


Figure 8. In-silico validation. (A) Expression pattern of MIAT in CRSwNP and control subjects. (B) Expression pattern of IRF4 in CRSwNP and control subjects. (C) Correlation analysis between MIAT and IRF4 in CRSwNP.

to be colonized with *Staphylococcus aureus* than controls and proteins *Staphylococcus aureus* as inducers of persistent type 2 airway inflammation^{67,68}. Neutrophils are essential for the clearance of bacteria either through phagocytosis or the formation of neutrophil extracellular traps (NETs)⁶⁹. The associations of eosinophilic infiltrate with CRSwNP and higher osteitis scores have been demonstrated⁷⁰. The inflammatory milieu disrupts the balance between osteoblasts and osteoclasts and leads to neo-osteogenesis⁷¹. Taken together, these results suggested that these DE-mRNAs are involved in CRSwNP biological processes and contribute to nasal polyps.

To better research the mechanism of CRSwNP, we first constructed a novel ceRNA regulatory network (including 21 lncRNAs, 8 miRNAs, and 8 mRNAs) involved in CRSwNP through bioinformatic analysis (Fig. 4B). Next, the hub lncRNA MIAT was obtained by hub analysis based on degree > 5 (Fig. 4C) (Table 2). Finally, based on coexpression of lncRNA-mRNA and its correlation analysis, a MIAT/miR-125a/IRF4 regulatory axis that fit the ceRNA pattern well was proposed (Fig. 4D,E). We verified the expression of MIAT and IRF4 in the extra validation GEO datasets (GSE36830 and GSE179265) (Figs. 5A,B and 8A,B), the upregulated expression of IRF4 was positive correlation with lncRNA MIAT (Fig. 8C), which further indicated that our screening results were reliable. MIAT was first identified in heart tissues and is known as myocardial infarction-associated transcript⁷². This lncRNA can regulate the expression of certain genes at the transcriptional or posttranscriptional levels. Constant studies have led to the fact that MIAT is involved in various diseases and cellular processes, mainly related to the activation of the inflammatory response⁷³. One study showed that the expression of MIAT increased in LPS-induced pneumonia, and deletion of MIAT protected against LPS-induced inflammation via the miR-147a/NKAP/NF- κ B axis⁷⁴. Another study showed that the expression of MIAT increased in the knee joint synovium and heart muscles of arthritic mice and macrophage inflammation⁷⁵. MiR-125a-5p has an important role in suppressing classical activation of macrophages while promoting alternative activation to promote anti-inflammatory responses⁷⁶. MiR-125a-5p is involved in the molecular mechanisms of rheumatoid arthritis⁷⁷ and osteoarthritis⁷⁸. IRF4 is a transcription factor that is related to the regulation of gene expression and the immune response. IRF4 plays an essential role in T cells, B cells, and myeloid cell differentiation⁷⁹. IRF4 expression is associated with many lymphoid malignancies and multiple myeloma⁸⁰. Additionally, the expression of IRF4 is increased in rheumatoid arthritis patients compared with healthy volunteers⁸¹. GSEA of IRF4 identified several immune cell infiltration and immune response-related pathways (Fig. 4F).

IRF4, a major regulator of M2 macrophage activation, has been demonstrated to be involved in the pathogenesis of allergic rhinitis and asthma^{82,83}. In this study, we found that IRF4 was markedly expressed in epithelial cells as well as macrophages in the nasal polyp tissues (Fig. 9A,B). We found that the production of IRF4 was upregulated in nasal polyps (Fig. 9C). The results provide strong support for our computational analyses, which suggests that IRF4 may be a potential biomarker for the selection of therapeutic strategies for CRSwNP.

To further explore the role of immune cell infiltration in CRSwNP, the CIBERSORT website was used to perform a comprehensive evaluation of 22 types of immune cell infiltration in CRSwNP patients (Fig. 6A). We found that increased infiltration of eosinophils and M2 macrophages may be related to the occurrence and development of CRSwNP. CRSwNP in the Caucasian population was categorized by a type 2 inflammatory response with enhanced tissue eosinophilia and higher levels of type 2 cytokines (interleukin (IL)-4, IL-5, and IL-13)¹⁵. However, non-ECRSwNP is more common in Asian populations, which have lower levels of IL-5 and increased levels of the type 1 cytokine IFN- γ when compared to nasal polyps from European patients⁸⁴. In the last two decades, there has been a trend toward increasing eosinophilic nasal polyps in Asian populations, possibly due to the rapid global adoption of a Western lifestyle⁸⁵. ECRSwNP demonstrates Th2 inflammation with higher recurrence and asthma comorbidity rates and a more frequent and severe presentation of clinical symptoms than non-ECRSwNP (Th1/Th17 inflammation)¹. Epithelial-derived innate cytokines, such as IL-25, IL-33, and thymic stromal lymphopoietin (TSLP), can stimulate eosinophils and their recruitment toward the impaired epithelium indirectly⁸⁶. Interestingly, eosinophils are locally activated in nasal polyp tissue to secrete protein and inflammatory mediators contributing to tissue damage and remodeling and further eosinophil recruitment⁸⁷. In addition to eosinophils, several other immune cell types are involved in the immunological mechanisms of CRSwNP, including macrophages, innate type 2 lymphoid cells, and mast cells¹⁵. Macrophages are phagocytic cells of the innate immune system, acting as a first line of defense along with the mucosal barrier. Activated macrophages are

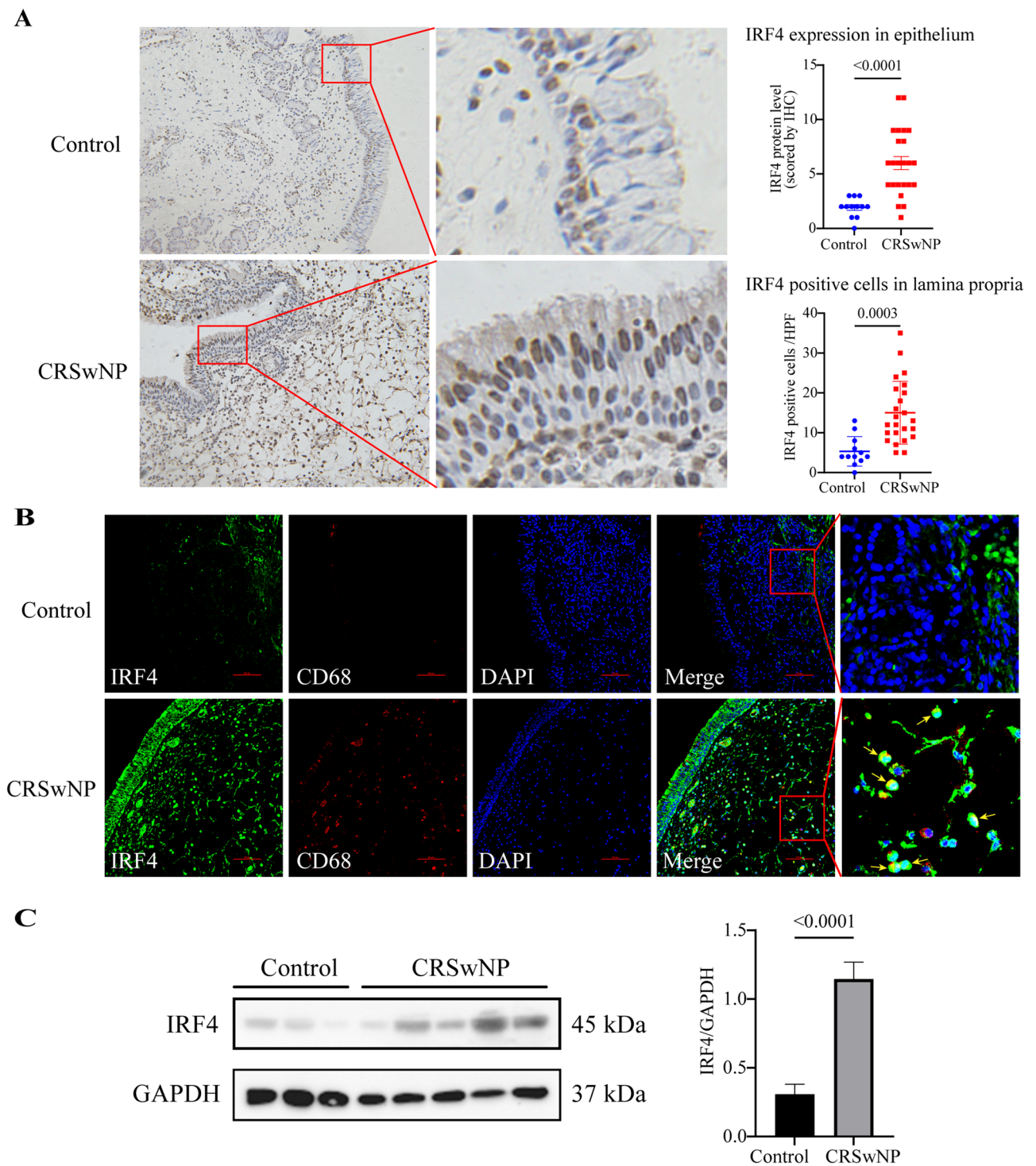


Figure 9. Experimental validation of the protein expression levels of IRF4. **(A)** Immunohistochemistry study demonstrated increased expression of IRF4 in the cytoplasm and nucleus, in nasal epithelial cells and inflammatory cells in lamina propria in nasal polyps. The representative photomicrographs are shown (original magnification $\times 200$). **(B)** Double immunofluorescence staining demonstrated IRF4 expression in CD68+ macrophages in lamina propria in nasal polyps. Arrows denote representative positive cells. **(C)** Representative blots of IRF4 protein expression in sinonasal mucosa.

subdivided into proinflammatory (M1) and anti-inflammatory (M2) macrophages⁸⁸. M1 macrophages support a Th1 response by expressing IL-1 β , IL-6, IL-12, and TNF- α , while M2 macrophages contribute to tissue repair and promote Th2 responses⁸⁹. There were positive correlations between the number of M2 macrophages and

clinical disease severity and inflammation in ECRSwNP⁹⁰. M2 macrophages can be alternatively activated by Th2 cytokines in tissue remodeling⁹¹. Our results further provided evidence that eosinophils and M2 macrophages could have possible therapeutic value in the treatment of patients with CRSwNP.

By analyzing the correlation between the ceRNA axis (lncRNA and mRNA) and immune cells, we found that MIAT was significantly positively correlated with resting dendritic cells (DCs) and M2 macrophages (Fig. 7A). IRF4 was significantly positively correlated with resting dendritic cells (Fig. 7B). MIAT acted as a ceRNA to regulate CD47 expression by sponging miR-149-5p in macrophages to inhibit efferocytosis in advanced atherosclerosis⁹². IRF4 is a critical transcription factor both for CD4+ T cells and DCs^{93,94}. IRF4 bound and activated IL-10 and IL-33 genes in DCs to promote Th2 differentiation and inflammation. DCs are used to bridge the innate and adaptive immune systems. DCs are innate immune cells that play a critical role in the host response to infection, as they recognize and respond to various antigens. Their defining role in adaptive immunity is to present exogenously introduced antigens in the context of MHC molecules for the activation of naive T cells⁹⁵. In addition to antigen presentation, cytokine production by DCs could affect T-cell differentiation and function⁹⁴. These results suggested that MIAT, IRF4, dendritic cells, and M2 macrophages play important roles in the immune response in patients with polyps. To the best of our knowledge, this is the first study to reveal the relationship between the ceRNA axis (lncRNA and mRNA) and infiltrating immune cells in CRSwNP. Our study revealed that the ceRNA network plays an important role in the pathogenesis of CRSwNP, which may represent potential diagnostic biomarkers and therapeutic targets. Our study also provided new insight into gene-immune cell regulatory mechanisms in CRSwNP. However, there are some limitations to this study. First, in this study, bioinformatics methods were used to identify differentially expressed genes (DEGs) between CRSwNP and normal tissues that can help reveal the pathological mechanism of CRSwNP at the genetic level, while Polisen et al. observed that nondifferentially expressed RNAs may also contribute to the spongy mechanism²⁷. We did not study these nondifferentially expressed ceRNAs in this study. Second, these datasets lacked clinical information, including comorbid asthma, IgE levels, Lund-Mackay CT scoring, and endoscopic nasal polyp scores, which could be used to assess the correlation between key genes and clinical features. Third, the number of samples used for the miRNA dataset was very low, and only lncRNA and mRNA biomarkers were validated in other datasets because there were no other publicly available miRNA datasets about the analyzed disease. Fourth, we did not analyze the relationship between miRNAs and ceRNAs (lncRNAs and mRNAs) due to the absence of the expression profiles on the same datasets for each RNA player. Finally, this study was based on open-access online databases and only experimentally validated the mRNA expression. In the future, we will validate the ceRNA network in cells and animal models.

Conclusion

In this study, we successfully constructed a potential lncRNA-miRNA-mRNA regulatory network in CRSwNP from multiple dimensions to provide a comprehensive understanding of the detailed molecular mechanisms underlying the pathogenesis of CRSwNP. Importantly, we confirmed a potential regulatory axis in which MIAT could regulate the expression of IRF4 by sponging miR-125a in CRSwNP. We also found that eosinophils and M2 macrophages may be involved in the occurrence and progression of CRSwNP. MIAT and IRF4 was significantly positively correlated with dendritic cells and M2 macrophages. We suppose that the MIAT/miR-125a/IRF4 axis may exert a critical role in the development and progression of CRSwNP.

Received: 19 January 2022; Accepted: 27 May 2022

Published online: 13 June 2022

References

1. Fokkens, W. J. *et al.* European position paper on rhinosinusitis and nasal polyps 2020. *Rhinology* **58**(Suppl S29), 1–464 (2020).
2. Orlandi, R. R. *et al.* International consensus statement on allergy and rhinology: Rhinosinusitis 2021. *Int. Forum Allergy Rhinol.* **11**(3), 213–739 (2021).
3. Bachert, C. & Akdis, C. A. Phenotypes and emerging endotypes of chronic rhinosinusitis. *J. Allergy Clin. Immunol. Pract.* **4**(4), 621–628 (2016).
4. Veloso-Teles, R. & Cerejeira, R. Endoscopic sinus surgery for chronic rhinosinusitis with nasal polyps: Clinical outcome and predictive factors of recurrence. *Am. J. Rhinol. Allergy* **31**(1), 56–62 (2017).
5. Khalmuratova, R., Park, J. W. & Shin, H. W. Immune cell responses and mucosal barrier disruptions in chronic rhinosinusitis. *Immune Netw.* **17**(1), 60–67 (2017).
6. Kim, J. W. *et al.* Histological and immunological features of non-eosinophilic nasal polyps. *Otolaryngol. Head Neck Surg.* **137**(6), 925–930 (2007).
7. Kim, Y. H. Establishing a therapeutic strategy targeting NF-kappaB in Asian patients with chronic rhinosinusitis with nasal polyps. *Allergy Asthma Immunol. Res.* **11**(6), 757–759 (2019).
8. Liu, Z. *et al.* Chinese society of allergy and chinese society of otorhinolaryngology-head and neck surgery guideline for chronic rhinosinusitis. *Allergy Asthma Immunol. Res.* **12**(2), 176–237 (2020).
9. Bachert, C., Gevaert, P. & Hellings, P. Biotherapeutics in chronic rhinosinusitis with and without nasal polyps. *J. Allergy Clin. Immunol. Pract.* **5**(6), 1512–1516 (2017).
10. Gurrola, J. & Borish, L. Chronic rhinosinusitis: Endotypes, biomarkers, and treatment response. *J. Allergy Clin. Immunol.* **140**(6), 1499–1508 (2017).
11. Hopkins, C. *et al.* Long-term outcomes from the English national comparative audit of surgery for nasal polyposis and chronic rhinosinusitis. *Laryngoscope* **119**(12), 2459–2465 (2009).
12. DeConde, A. S. *et al.* Prevalence of polyp recurrence after endoscopic sinus surgery for chronic rhinosinusitis with nasal polyposis. *Laryngoscope* **127**(3), 550–555 (2017).
13. Bachert, C. *et al.* EUFOREA expert board meeting on uncontrolled severe chronic rhinosinusitis with nasal polyps (CRSwNP) and biologics: Definitions and management. *J. Allergy Clin. Immunol.* **147**(1), 29–36 (2021).
14. Hopkins, C. Chronic rhinosinusitis with nasal polyps. *N. Engl. J. Med.* **381**(1), 55–63 (2019).

15. Stevens, W. W., Schleimer, R. P. & Kern, R. C. Chronic rhinosinusitis with nasal polyps. *J. Allergy Clin. Immunol. Pract.* **4**(4), 565–572 (2016).
16. Bequignon, E. *et al.* Pathogenesis of chronic rhinosinusitis with nasal polyps: Role of IL-6 in airway epithelial cell dysfunction. *J. Transl. Med.* **18**(1), 136 (2020).
17. Jacquier, A. The complex eukaryotic transcriptome: Unexpected pervasive transcription and novel small RNAs. *Nat. Rev. Genet.* **10**(12), 833–844 (2009).
18. Liu, Y. *et al.* Role of microRNAs, circRNAs and long noncoding RNAs in acute myeloid leukemia. *J. Hematol. Oncol.* **12**(1), 51 (2019).
19. Filipowicz, W., Bhattacharyya, S. N. & Sonenberg, N. Mechanisms of post-transcriptional regulation by microRNAs: Are the answers in sight?. *Nat. Rev. Genet.* **9**(2), 102–114 (2008).
20. Zhang, X. H. *et al.* Overexpression of miR-125b, a novel regulator of innate immunity, in eosinophilic chronic rhinosinusitis with nasal polyps. *Am. J. Respir. Crit. Care Med.* **185**(2), 140–151 (2012).
21. Liu, C. C. *et al.* Micro124-mediated AHR expression regulates the inflammatory response of chronic rhinosinusitis (CRS) with nasal polyps. *Biochem. Biophys. Res. Commun.* **500**(2), 145–151 (2018).
22. Zhang, J., Han, L. & Chen, F. Let-7a-5p regulates the inflammatory response in chronic rhinosinusitis with nasal polyps. *Diagn. Pathol.* **16**(1), 27 (2021).
23. Ponting, C. P., Oliver, P. L. & Reik, W. Evolution and functions of long noncoding RNAs. *Cell* **136**(4), 629–641 (2009).
24. Salmena, L. *et al.* A ceRNA hypothesis: The Rosetta Stone of a hidden RNA language?. *Cell* **146**(3), 353–358 (2011).
25. Lin, J. *et al.* Long noncoding RNA TUG1 promotes airway smooth muscle cells proliferation and migration via sponging miR-590-5p/FGF1 in asthma. *Am. J. Transl. Res.* **11**(5), 3159–3166 (2019).
26. Conte, F. *et al.* An overview of the computational models dealing with the regulatory ceRNA mechanism and ceRNA deregulation in cancer. *Methods Mol. Biol.* **2324**, 149–164 (2021).
27. Polisenio, L. *et al.* A coding-independent function of gene and pseudogene mRNAs regulates tumour biology. *Nature* **465**(7301), 1033–1038 (2010).
28. Conte, F. *et al.* Role of the long non-coding RNA PVT1 in the dysregulation of the ceRNA-ceRNA network in human breast cancer. *PLoS ONE* **12**(2), e0171661 (2017).
29. Yang, X. Z. *et al.* LINC01133 as ceRNA inhibits gastric cancer progression by sponging miR-106a-3p to regulate APC expression and the Wnt/beta-catenin pathway. *Mol. Cancer* **17**(1), 126 (2018).
30. Xu, G. *et al.* LncRNA MIR194-2HG promotes cell proliferation and metastasis via regulation of miR-1207-5p/TCF19/Wnt/beta-catenin signaling in liver cancer. *Onco Targets Ther.* **13**, 9887–9899 (2020).
31. Yue, L. *et al.* Long noncoding RNA Linc00632 inhibits interleukin-13-induced inflammatory cytokine and mucus production in nasal epithelial cells. *J. Innate Immun.* **12**(1), 116–128 (2020).
32. Wang, W. *et al.* Transcriptome analysis reveals distinct gene expression profiles in eosinophilic and noneosinophilic chronic rhinosinusitis with nasal polyps. *Sci. Rep.* **6**, 26604 (2016).
33. Wang, R. *et al.* The correlation of long non-coding RNA NEAT1 and its targets microRNA (miR)-21, miR-124, and miR-125a with disease risk, severity, and inflammation of allergic rhinitis. *Medicine (Baltimore)* **100**(4), e22946 (2021).
34. Davis, S. & Meltzer, P. S. GEOquery: A bridge between the gene expression omnibus (GEO) and BioConductor. *Bioinformatics* **23**(14), 1846–1847 (2007).
35. Peng, Y. *et al.* Whole-transcriptome sequencing reveals heightened inflammation and defective host defence responses in chronic rhinosinusitis with nasal polyps. *Eur. Respir. J.* **54**(5), 1900732 (2019).
36. Seshadri, S. *et al.* Reduced expression of antimicrobial PLUNC proteins in nasal polyp tissues of patients with chronic rhinosinusitis. *Allergy* **67**(7), 920–928 (2012).
37. Nakayama, T. *et al.* Inflammatory molecular endotypes of nasal polyps derived from White and Japanese populations. *J. Allergy Clin. Immunol.* **149**(4), 1296–1308 (2022).
38. Yu, J. *et al.* Gene expression profiles of circular RNAs and MicroRNAs in chronic rhinosinusitis with nasal polyps. *Front. Mol. Biosci.* **8**, 643504 (2021).
39. Love, M. I., Huber, W. & Anders, S. Moderated estimation of fold change and dispersion for RNA-seq data with DESeq2. *Genome Biol.* **15**(12), 550 (2014).
40. Ritchie, M. E. *et al.* limma powers differential expression analyses for RNA-sequencing and microarray studies. *Nucleic Acids Res.* **43**(7), e47 (2015).
41. Yu, G. *et al.* clusterProfiler: An R package for comparing biological themes among gene clusters. *OMICS* **16**(5), 284–287 (2012).
42. Kanehisa, M. *et al.* The KEGG resource for deciphering the genome. *Nucleic Acids Res.* **32**, D277–280 (2004).
43. Subramanian, A. *et al.* Sub set enrichment analysis: A knowledge-based approach for interpreting genome-wide expression profiles. *Proc Natl. Acad. Sci. U.S.A.* **102**(43), 15545–15550 (2005).
44. Cline, M. S. *et al.* Integration of biological networks and gene expression data using Cytoscape. *Nat. Protoc.* **2**(10), 2366–2382 (2007).
45. Newman, A. M. *et al.* Robust enumeration of cell subsets from tissue expression profiles. *Nat. Methods* **12**(5), 453–457 (2015).
46. Ginestet, C. ggplot2: Elegant graphics for data analysis. *J. R. Stat. Soc. Ser. Stat. Soc.* **174**, 245–245 (2011).
47. Friendly, M. Corrgrams: Exploratory displays for correlation matrices. *Am. Stat.* **56**(4), 316–324 (2002).
48. Robinson, M. D., McCarthy, D. J. & Smyth, G. K. edgeR: A Bioconductor package for differential expression analysis of digital gene expression data. *Bioinformatics* **26**(1), 139–140 (2010).
49. Pistochini, A. *et al.* Multiple gene expression profiling suggests epithelial dysfunction in polypoid chronic rhinosinusitis. *Acta Otorhinolaryngol. Ital.* **39**(3), 169–177 (2019).
50. Biggs, T. C. *et al.* Immunological profiling of key inflammatory drivers of nasal polyp formation and growth in chronic rhinosinusitis. *Rhinology* **57**(5), 336–342 (2019).
51. Yang, P. *et al.* Agonist of PPAR-gamma reduced epithelial-mesenchymal transition in eosinophilic chronic rhinosinusitis with nasal polyps via inhibition of high mobility group Box1. *Int. J. Med. Sci.* **16**(12), 1631–1641 (2019).
52. Okada, N. *et al.* Distinct gene expression profiles and regulation networks of nasal polyps in eosinophilic and non-eosinophilic chronic rhinosinusitis. *Int. Forum Allergy Rhinol.* **8**(5), 592–604 (2018).
53. Liu, T., Sun, Y. & Bai, W. The role of epigenetics in the chronic sinusitis with nasal polyp. *Curr. Allergy Asthma Rep.* **21**(1), 1 (2020).
54. Zhou, X. *et al.* Identification of key modules, hub genes, and noncoding RNAs in chronic rhinosinusitis with nasal polyps by weighted gene coexpression network analysis. *Biomed Res. Int.* **2020**, 6140728 (2020).
55. Chu, K. J. *et al.* Whole-transcriptome sequencing identifies key differentially expressed mRNAs, miRNAs, lncRNAs, and circRNAs associated with CHOL. *Mol. Ther. Nucleic Acids* **21**, 592–603 (2020).
56. Jing, S. *et al.* Identification of a new pseudogenes/lncRNAs-hsa-miR-26b-5p-COL12A1 competing endogenous RNA network associated with prognosis of pancreatic cancer using bioinformatics analysis. *Aging (Albany NY)* **12**(19), 19107–19128 (2020).
57. Huang, R. *et al.* The construction and comprehensive analysis of ceRNA networks and tumor-infiltrating immune cells in bone metastatic melanoma. *Front. Genet.* **10**, 828 (2019).
58. Hulse, K. E. *et al.* Pathogenesis of nasal polyposis. *Clin. Exp. Allergy* **45**(2), 328–346 (2015).
59. Bachert, C. *et al.* Adult chronic rhinosinusitis. *Nat. Rev. Dis. Primers* **6**(1), 86 (2020).

60. Didehdar, M. *et al.* An overview of possible pathogenesis mechanisms of *Alternaria alternata* in chronic rhinosinusitis and nasal polyposis. *Microb. Pathog.* **155**, 104905 (2021).
61. Scadding, G. K. & Scadding, G. W. Innate and adaptive immunity: ILC2 and Th2 cells in upper and lower airway allergic diseases. *J. Allergy Clin. Immunol. Pract.* **9**(5), 1851–1857 (2021).
62. Peterson, S. *et al.* Increased expression of CC chemokine ligand 18 in patients with chronic rhinosinusitis with nasal polyps. *J. Allergy Clin. Immunol.* **129**(1), 119–127 (2012).
63. Li, C.C. *et al.* Impact of matrix metalloproteinases 11 gene variants on urothelial cell carcinoma development and clinical characteristics. *Int. J. Environ. Res. Public Health* **17**(2), 475 (2020).
64. Luo, M. J. *et al.* Fasting before or after wound injury accelerates wound healing through the activation of pro-angiogenic SMO1 and SCG2. *Theranostics* **10**(8), 3779–3792 (2020).
65. Kaur, A. *et al.* Remodeling of the collagen matrix in aging skin promotes melanoma metastasis and affects immune cell motility. *Cancer Discov.* **9**(1), 64–81 (2019).
66. Pang, X. *et al.* Identification of SPP1 as an extracellular matrix signature for metastatic castration-resistant prostate cancer. *Front. Oncol.* **9**, 924 (2019).
67. Van Zele, T. *et al.* Staphylococcus aureus colonization and IgE antibody formation to enterotoxins is increased in nasal polyposis. *J. Allergy Clin. Immunol.* **114**(4), 981–983 (2004).
68. Teufelberger, A. R. *et al.* Staphylococcus aureus orchestrates type 2 airway diseases. *Trends Mol. Med.* **25**(8), 696–707 (2019).
69. Wang, H., Pan, L. & Liu, Z. Neutrophils as a protagonist and target in chronic rhinosinusitis. *Clin. Exp. Otorhinolaryngol.* **12**(4), 337–347 (2019).
70. Snidvongs, K., Sacks, R. & Harvey, R. J. Osteitis in chronic rhinosinusitis. *Curr. Allergy Asthma Rep.* **19**(5), 24 (2019).
71. Kholmuratova, R. *et al.* Evaluation of neo-osteogenesis in eosinophilic chronic rhinosinusitis using a nasal polyp murine model. *Allergy Asthma Immunol. Res.* **12**(2), 306–321 (2020).
72. Ishii, N. *et al.* Identification of a novel non-coding RNA, MIAT, that confers risk of myocardial infarction. *J. Hum. Genet.* **51**(12), 1087–1099 (2006).
73. Zhang, J. *et al.* C-myc contributes to the release of Müller cells-derived proinflammatory cytokines by regulating lncRNA MIAT/XNIP pathway. *Int. J. Biochem. Cell Biol.* **114**, 105574 (2019).
74. Liu, M. *et al.* Silencing of lncRNA MIAT alleviates LPS-induced pneumonia via regulating miR-147a/NKAP/NF-kappaB axis. *Agng (Albany NY)* **13**(2), 2506–2518 (2020).
75. Wang, Z. *et al.* lncRNA MIAT downregulates IL-1beta, TNF-a to suppress macrophage inflammation but is suppressed by ATP-induced NLRP3 inflammasome activation. *Cell Cycle* **20**(2), 194–203 (2021).
76. Banerjee, S. *et al.* miR-125a-5p regulates differential activation of macrophages and inflammation. *J. Biol. Chem.* **288**(49), 35428–35436 (2013).
77. Murata, K. *et al.* Comprehensive microRNA analysis identifies miR-24 and miR-125a-5p as plasma biomarkers for rheumatoid arthritis. *Plos One* **8**(7), e69118 (2013).
78. Shen, P. *et al.* CircCDK14 protects against Osteoarthritis by sponging miR-125a-5p and promoting the expression of Smad2. *Theranostics* **10**(20), 9113–9131 (2020).
79. Nam, S. & Lim, J. S. Essential role of interferon regulatory factor 4 (IRF4) in immune cell development. *Arch. Pharmacol. Res.* **39**(11), 1548–1555 (2016).
80. Shaffer, A. L. *et al.* IRF4: Immunity. Malignancy! Therapy?. *Clin. Cancer Res.* **15**(9), 2954–2961 (2009).
81. Rodriguez-Carrio, J. *et al.* IRF4 and IRGs delineate clinically relevant gene expression signatures in systemic lupus erythematosus and rheumatoid arthritis. *Front. Immunol.* **9**, 3085 (2018).
82. Bruhn, S. *et al.* Increased expression of IRF4 and ETS1 in CD4+ cells from patients with intermittent allergic rhinitis. *Allergy* **67**(1), 33–40 (2012).
83. Chen, X., Gao, Y. D. & Yang, J. Elevated interferon regulatory factor 4 levels in patients with allergic asthma. *J. Asthma* **49**(5), 441–449 (2012).
84. Zhang, N. *et al.* Different types of T-effector cells orchestrate mucosal inflammation in chronic sinus disease. *J. Allergy Clin. Immunol.* **122**(5), 961–968 (2008).
85. Kim, S. J. *et al.* Changes in histological features of nasal polyps in a Korean population over a 17-year period. *Otolaryngol. Head Neck Surg.* **149**(3), 431–437 (2013).
86. Zhang, N. *et al.* Barrier function of the nasal mucosa in health and type-2 biased airway diseases. *Allergy* **71**(3), 295–307 (2016).
87. Bochner, B. S. & Stevens, W. W. Biology and function of eosinophils in chronic rhinosinusitis with or without nasal polyps. *Allergy Asthma Immunol. Res.* **13**(1), 8–22 (2021).
88. Murray, P. J. & Wynn, T. A. Obstacles and opportunities for understanding macrophage polarization. *J. Leukoc. Biol.* **89**(4), 557–563 (2011).
89. Barros, M. H. *et al.* Macrophage polarisation: An immunohistochemical approach for identifying M1 and M2 macrophages. *PLoS ONE* **8**(11), e80908 (2013).
90. Yao, Y. *et al.* Increased expression of TIPE2 in alternatively activated macrophages is associated with eosinophilic inflammation and disease severity in chronic rhinosinusitis with nasal polyps. *Int. Forum Allergy Rhinol.* **7**(10), 963–972 (2017).
91. Krysko, O. *et al.* Alternatively activated macrophages and impaired phagocytosis of *S. aureus* in chronic rhinosinusitis. *Allergy* **66**(3), 396–403 (2011).
92. Ye, Z. M. *et al.* lncRNA MIAT sponges miR-149-5p to inhibit efferocytosis in advanced atherosclerosis through CD47 upregulation. *Cell Death Dis.* **10**(2), 138 (2019).
93. Wu, J. *et al.* Ablation of transcription factor IRF4 promotes transplant acceptance by driving allogenic CD4(+) T cell dysfunction. *Immunity* **47**(6), 1114–1128 (2017).
94. Williams, J. W. *et al.* Transcription factor IRF4 drives dendritic cells to promote Th2 differentiation. *Nat. Commun.* **4**, 2990 (2013).
95. Collin, M. & Bigley, V. Human dendritic cell subsets: An update. *Immunology* **154**(1), 3–20 (2018).

Author contributions

H.Y. and F.Y. collected the data and wrote the paper. Q.X., J.C. and Y.L. analyzed the data and wrote the paper. J.C. and Q.X. conceived and designed this study and wrote the paper. W.K. and Y.W. revised the paper. All authors read and approved the final manuscript.

Funding

Scientific research project of Shihezi University (ZZZC2021105), Bethune Charitable Foundation (BQE-TY-SSPC (8)-E-01), Health Commission of Hubei Province scientific research project (WJ2021M250).

Competing interests

The authors declare no competing interests.

Additional information

Correspondence and requests for materials should be addressed to W.K. or Y.W.

Reprints and permissions information is available at www.nature.com/reprints.

Publisher's note Springer Nature remains neutral with regard to jurisdictional claims in published maps and institutional affiliations.



Open Access This article is licensed under a Creative Commons Attribution 4.0 International License, which permits use, sharing, adaptation, distribution and reproduction in any medium or format, as long as you give appropriate credit to the original author(s) and the source, provide a link to the Creative Commons licence, and indicate if changes were made. The images or other third party material in this article are included in the article's Creative Commons licence, unless indicated otherwise in a credit line to the material. If material is not included in the article's Creative Commons licence and your intended use is not permitted by statutory regulation or exceeds the permitted use, you will need to obtain permission directly from the copyright holder. To view a copy of this licence, visit <http://creativecommons.org/licenses/by/4.0/>.

© The Author(s) 2022